AADE-20-FTCE-109

Transient Pressure Behavior in Wellbores due to Fluid Gelation

Osman K. Gunes and Evren Ozbayoglu, The University of Tulsa

Abstract

Drilling fluids are desired to develop a gelled structure to improve cutting transport ability during circulation, and to prevent precipitation of cuttings and other constituents in static or no circulation conditions. Despite these advantages, gelation can be detrimental when the circulation is resumed after a period of time due to any operational circumstances since additional energy is required to overcome such a gelled structure. Resultant pressure peaks could fracture the formation, leading to possible safety risks and tremendous cost. In particular, this is important for complex drilling operations with narrow geo-pressure windows, such as those in offshore wells. For these reasons, pressure peaks created when circulation is resumed and the accompanying transient pressure behavior are of significant importance. This study focuses on predicting pressure peaks when pumps are restarted after a static period of time. It includes laboratory and flow loop experiments which enable investigation of such behavior in both small and large scales. Two models are also proposed to predict transient shear stress behavior which permits determination of pressure gradient by considering different shear rates after a variety of resting time intervals. Understanding potential pressure peaks is expected to help if extra care is required when restarting the circulation. Also, predicting such transient pressure behavior might be useful for an automated drilling control system to avoid generating downhole pressure above fracturing pressure gradient of the open hole section.

Introduction

One of the concerns in drilling operations is the falling of cuttings or other dissolved or undissolved constituents in the drilling fluid in case of no circulation situations. In order to avoid precipitation of cuttings in the annulus during the pump off, drilling fluids are designed to take form of a gelled structure. On the other hand, this structure, which is important for effective cutting transport and cutting suspension in the drilling fluid, could turn into a trouble due to its complex time and shear dependent behavior. The fluid with gelled structure, developed during pump off condition, has both elastic and viscous characteristics, which makes it more complicated. Aforementioned gelation behavior leads to troublesome pressure peaks on the wellbore when it is attempted to restart the circulation to continue the drilling operation (Gandelman et al. 2007). These surge pressures are of great potential to induce formation fracture which may also cause lost circulation problems especially in the wells which narrow operating windows exist such as offshore, high pressure-high temperature (HPHT) and extended reach wells.

A series of laboratory experiments with a conventional viscometer (Ofite Model 900) and a high-precision rheometer (Anton Paar Physica MCR 301) has been carried out. Shear stress responses of two WBM due to gel breaking activity have been investigated thoroughly. Fluid displacement tests in a flow loop were also carried out in a vertical concentric annulus to investigate pressure response in a large scale system.

Two different models which account for both shear rate and shear history are proposed to predict transient shear stress response observed when the gel breaking takes place. This helps with comparison of obtaining model parameters in terms of simplicity and accessibility. Modeling shear stress behavior enables estimation of transient pressure behavior by using the parallel plate approximation method.

Experiments

The study is composed of both rheometer and flow loop experiments. All experiments were carried out at room temperature of 24 ^{o}C. Also, fluid density was measured as 8.55 ppg or 1024.51 kg/m^3.

Laboratory Experiments

Variety of tests were conducted with two different WBM fluids; i) a high yield fluid, and ii) a low yield fluid. High yield stress is achieved by adding soda ash to increase its pH. The pH values of the solutions were measured in the range of 8 to 10. Bentonite and polymer (Xanplex-D) were slowly added to the solution to avoid flocculation, respectively. Low yield fluid was prepared by applying a similar procedure, but with no soda ash added. Specific formulations of the fluids are given in Table 1. The fluid samples were also allowed to be cured for 16 hours at room temperature (24 ^{o}C) to allow clays to swell. The fluid was pre-sheared for ten minutes with a standard mixer to ensure homogeneity after 16 hours of curing period. Bentonite solutions were known to be thixotropic (Bekkour 2005). Thus, after the fluid was transferred into the measurement cup, every test begun with pre-shearing at 300 s^{-1} for 60 seconds to ensure breaking intermolecular structure. To obtain consistent and

reliable results, similar fluid preparation protocol was applied to all fluid samples. Also, "fresh" fluid samples were used for each test.

Rheological characterization experiments such as conventional constant shear rate tests, oscillatory amplitude sweep tests (OAST) and stress overshoot tests (SOT) were performed to characterize the fluid. Ofite Model 900 viscometer was used to obtain conventional viscometer dial readings at different rotational speeds. This data is tabulated and presented in Table 4. Also, the conventional viscometer was employed to measure gel strength of the fluids after 10 seconds, 1 min., 10 min., 30 min. and 60 min. of resting times to associate the model with parameters which can be easily accessible and obtained on the rig.

OASTs are known to provide information about the stability of the structure of the fluids which is related to the gel structure development. Viscoelastic behavior of the fluid can also be observed with the help of these tests (Mezger 2011). OAST and SOT were conducted using Anton Paar MCR301 rheometer. Based on Figure 6, it can be stated that both fluids (WBM#1 and WBM#2) shows that G' (storage modulus related to elastic characteristic) is higher than G'' (loss modulus related to viscous characteristic) which implies that they have viscoelastic characteristics. At low deformation, both G' and G'' are constant which means the sample structure is undisturbed.

Viscoelastic fluid is suddenly exposed to a shear rate during start-up flow. Shear stress generated by this transient deformation shows an initial overshoot before it reaches a steady-state shear stress and associated steady-state deformation. Thus, this behavior is called stress overshoot (Steffe 1996). Various SOTs were conducted by applying different resting time periods to study the development of shear stress response due to a sudden shear rate employed.

Fluid Displacement Experiments

Several flow loop tests are conducted to observe the development and severity of pressure peaks associated with different gelation times at different flow rates.

Pressure readings are recorded through the vertical concentric annular test section. The total vertical length of the test section is approximately 3 meters. However, pressure readings are recorded by two point pressure gauges which are 1.54 feet apart from each other, located at fully developed section. This vertical part has a 2" ID steel pipe with 0.5" OD stainless steel pipe inside. A fluid sample is circulated by using the Moyno Pump, which is a progressive cavity pump with maximum flow rate capacity of 20 gpm. The flow rate is obtained by circulating the fluid through the mass flow meter located at the outlet of the pump. The facility also enables temperature control with the horizontal heat exchanger section as a part of the flow loop. At the junction in between horizontal bypass and vertical test sections of the flow loop, a pneumatic valve, which is operated by a computer program, is used to divert the fluid into the section of interest. Schematic diagram of DTF (Dynamic testing facility) flow loop used in this study is presented in Figure 7.

The design of the facility enabled to trap the fluid and to allow it to rest in the vertical section for a specific period of time, while the circulation was continued in horizontal bypass line to shear the fluid and maintain the steady state fluid properties. After a desired resting time was achieved, the valve was actuated to divert all fluid into the vertical section to displace the fluid rested for a predetermined time. Also, all fluid displacement experiments were conducted at the same valve speed for the sake of consistency.

To make sure that the fluid was mixed thoroughly, the fluids were prepared in buckets, 24 gallons in total, and let it cured for 16 hours to swell completely before mixing it in the tank on the flow loop. Schematic diagram of the flow loop is given in Figure 7. After the mixing process, it was circulated through the flow loop for at least 30 minutes to ensure complete mixing. For the flow loop experiments, it was necessary to process the data to acquire pressure loss gradient.

Several tests were conducted with both WBM fluids. To investigate the effect of resting time on pressure reading during displacement of gelled fluid with the non-gelled one, several resting times, such as 5 min., 15 min., 30 min. and 60 min., were employed. Two flow rates, i.e., 5 and 10 gpm, were also used to observe the influence of flow rate on the displacement process. The resultant pressure behavior is provided in Figure 11 through Figure 18. Please note that experimental results for different resting times were combined and plotted on a single graph for illustrative purposes. Each test started with zero pressure loss, indicating no circulation, and a pressure peak was observed when the valve was switched. After the fluid was fully displaced, they all converged to the steady state pressure loss gradient.

Results and discussion

Fluid Characterization

The steady state rheological behavior of the fluids is characterized by the three parameter Herschel-Bulkley, also known as yield-power-law (YPL), and they are provided in Table 1. Steady shear tests were performed on Anton Paar MCR301 rheometer to construct the flow curves, and model parameters were determined by conventional curve fitting techniques. Flow curves are presented in Figure 8.

$$\tau = \tau_y + K\dot{\gamma}^m \quad (1)$$

Table 1 YPL parameters and compositions of WBM fluids

Case Number	Composition (Quantity for 1 bbl)	τ_y (Pa)	K (Pa*s^m)	m
WBM#1 (low yield fluid)	15 lb Bentonite 2 lb Xanplex-D	0.91	0.45	0.60
WBM#2 (high yield fluid)	15 lb Bentonite 2 lb Xanplex-D 0.25 lb Soda Ash	6.30	1.57	0.46

Fitting equations

Modified Leider & Bird Model*

Leider & Bird (1974) provide an empirical correlation with

rheological properties related to the first normal stress difference and the shear rate. This equation is expressed as a function of time and shear rate applied. General Leider & Bird equation is represented by Power Law steady shear stress $\{\tau_{(eq\ or\ \infty)}=K(\dot{\gamma})^m\}$, which can be modified by replacing it with Herschel-Bulkley fluid model, since bentonite solutions are known to be characterized by YPL (Bekkour et al. 2005):

$$\tau = f(\dot{\gamma},t) = (\tau_y + K(\dot{\gamma})^m)\left[1 + (b\dot{\gamma}t - 1)\exp\left(-\frac{t}{am\lambda}\right)\right] \quad (2)$$

where

$$\lambda = \left(\frac{K_n}{2K}\right)^{\frac{1}{n_n - m}}$$

Please note that *a* and *b* are adjustable model parameters. Also, λ is a time constant with K_n, n_n, and YPL parameters τ_y, K and m. K_n and n_n are called "first normal stress parameters" to be obtained experimentally or from equations available in the literature. In this study, equations 3 & 4 (Steller 2016) are used to calculate associated first normal stresses. It is recommended that the parameters K_n and n_n in equation-3 can be obtained by fitting N_1 values determined through equation 4 by using steady shear stress data at shear rates lower than 100 s^{-1}.

$$N_1 = \sigma_{11} - \sigma_{22} = K_n(\dot{\gamma})^{n_n} \quad (3)$$

$$N_1 = 12\tau(\dot{\gamma})\sqrt{1-m}\,(1+m)^{-4} \quad (4)$$

In addition to Modified Leider & Bird Model, previous attempt performed by Bekkour showed that this model only provides a satisfactory match with the SOT data for short rest times and low shearing conditions. Thus, in this study τ_y is replaced with time dependent yield stress which is defined in Equation 5. This equation implies that τ_y (t) is equal to the "static yield stress" (τ_{gel}) when time is zero or when the fluid is not sheared. Also, it approaches to steady state yield stress ($\tau_{y(ss)}$) which is referred as "dynamic yield stress" in the literature when time goes to infinity. Modified Leider & Bird model parameters for WBM#1 and WBM#2 are presented in Table 2.

Table 2 Modified Leider & Bird parameters for WBM#1 and WBM#2

Case #	$\dot{\gamma}(s^{-1})$	m	n_n	K (Pa.s^m)	K_n(Pa.s^m)	$\tau_{y(ss)}$ (Pa)	a	b
WBM#1	10.22	0.60	0.17	0.45	2.37	0.91	0.9	1.4
WBM#2	10.22	0.46	0.10	1.58	15.75	6.30	15	1.5

$$\tau_y(t) = \frac{\tau_{gel} - \tau_{y(ss)}}{1+t} + \tau_{y(ss)} \quad (5)$$

$$\lim_{t\to\infty} \tau_c(t) = \lim_{t\to\infty}\left[\frac{\tau_{gel} - \tau_y(ss)}{1+t} + \tau_y(ss)\right] \quad (6)$$

$$\tau_y(t=0) = \tau_{gel} \quad (7)$$

$$\tau_y(t=\infty) = \tau_y(ss) \quad (8)$$

Several stress overshoot tests (SOTs) were carried out with variety of predetermined resting time periods to investigate the evolution of the suspension structure with different resting times under controlled shear rate which is selected to be 10.22 s^{-1} representing fluid circulation shear rate in the riser annulus (Gandelman et al. 2007).

Figure 2 & Figure 3 show comparison of SOTs and Modified Leider & Bird model with time dependent yield stress. During all model fits for both WBM#1 and WBM#2, model parameters are kept constant to be convenient, since same shear rate ($\dot{\gamma}$=10.22 s^{-1}) and similar compositions are employed. Please note that only different parameter in both graphs is the aforementioned static yield stress, which is directly proportional to the resting time. In other words, static yield stress increases with increasing resting time period employed. Also, it can be stated that aforementioned time dependent yield stress values assumed for different resting times (τ_{gel}) are very close to the gel strength data obtained using conventional Ofite Model 900 viscometer at 3 rpm. Comparison of 3 rpm readings and model determined time dependent yield stresses for different resting intervals are presented in Figure 9 Figure 10 for WBM#1 and WBM#2, respectively.

Viscoelastic Model

Viscoelasticity is pointed out as the fact that it is a complex characteristic with solid like behavior to prevent cuttings, weighing agents and chemical additives from precipitating when pump is in off condition meaning no circulation (Maxey 2007). The fluids with this complex characteristic have both solid-like and fluid-like behavior simultaneously. In other words, they have characteristics of both elastic and viscous deformation.

In this study, as the "second model", in order to explain complex viscoelastic behavior causing transient pressure behavior, Burgers Model is considered. In 1935, Burgers proposed a model to describe viscoelastic characteristics of a fluid. Figure 1 illustrates the Burgers material which is composed of both Maxwell and Kelvin/Voigt models. Spring and dashpot components are in the form of Maxwell Model which includes spring and dashpot in series (component 1 and 3), and Kelvin/Voigt Model with spring and dashpot in parallel (component 2). To be more specific, the spring represents the elastic behavior of the fluid in the early time; Kelvin/Voigt model, which is connected in parallel, simulates the viscoelastic behavior in the transition time; and the dashpot represents the purely viscous behavior in the steady state conditions.

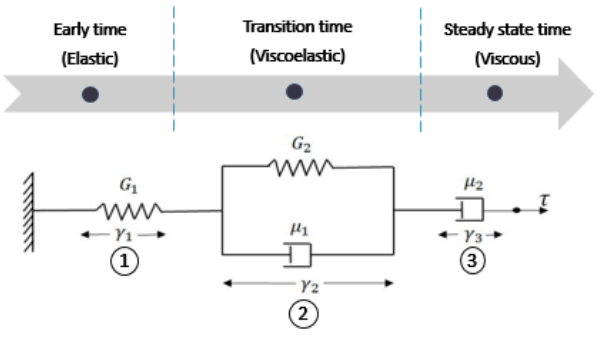

Figure 1 Schematic diagram of Burgers material

Strain-stress relationship for this model is given as (Altindal et al. 2017):

$$\tau = q_1\dot{\gamma} + \frac{e^{-Bt}C\left\{\cosh(At)+\frac{p_2\sinh(At)\left[\frac{q_1\tau_0+G_0\dot{\gamma}q_2-G_0\dot{\gamma}p_1q_1}{C}-B\right]}{Ap_2}\right\}}{G_0p_2} \quad (9)$$

where

$$A = \frac{\left(\frac{p_1^2}{4}-p_2\right)^{0.5}}{p_2}\ ,\ B = \frac{p_1}{2p_2}\ ,\ C = q_2\tau_0 - G_0\dot{\gamma}p_2q_1$$

$$p_1 = \frac{\mu_1G_1+\mu_2G_1+\mu_2G_2}{G_1G_2}\ ,\ p_2 = \frac{\mu_1\mu_2}{G_1G_2}$$

$$q_1 = \mu_2\ ,\ q_2 = \frac{\mu_1\mu_2}{G_2}$$

Equation 9 describes the shear stress behavior of a drilling fluid as a function of time and shear rate. It also accounts for the elastic effects of the drilling fluid with the spring constants G_1 and G_2 and the viscous effects with the dashpot constants μ_1 and μ_2. The equation has four unknowns, which are p_1, p_2, q_1 and q_2 to be determined by applying regression techniques to SOT experimental data. The fitting practice is repeated for all data sets obtained by SOTs to predict the shear stress response when the fluid is subjected to a shear rate after a specific rest time. Please note that the raw data is refined by discarding the intervals dominated by inertial effects which can be observed in the very early times of SOTs. For the fluids employed in this study, the model parameters are presented in Table 3.

Table 3 Viscoelastic parameters for WBM#1 and WBM#2 for variety of resting times

Resting Time	VE parameters							
	p1		q1		p2		q2	
	WBM #1	WBM #2	WBM #1	WBM #2	WBM #1	WBM #2	WBM #1	WBM #2
10 sec.	0.6637	0.3700	0.3200	1.2400	0.0180	0.0104	0.1800	0.5000
1 min.	0.6637	0.3700	0.3200	1.2400	0.0171	0.0105	0.2400	0.6300
10 min.	0.6637	0.3700	0.3200	1.2400	0.0173	0.0134	0.3800	0.8700
30 min.	0.6637	0.3700	0.3200	1.2400	0.0240	0.0147	0.4800	1.0000
60 min.	0.6637	0.3700	0.3200	1.2400	0.0212	0.0168	0.5500	1.2400

Sample Scenario

For illustration purposes, it is assumed that a drilling operation is performed with 8 ½ wellbore with a 4 ½ drill string using WBM#1 and WBM#2 fluids, respectively. It is assumed that the pumps are restarted after the well has rested for 30 minutes due to an operational circumstance. The pump rates at start-up are set to 100 and 300 gpm, respectively. Annular space is represented by using parallel plate approximation (Bjørkevoll et al. 2003):

$$\frac{\Delta P}{\Delta L} = \frac{4\tau_w}{D_o - D_i} \quad (10)$$

τ_w is determined from the proposed models by first calculating the associated wall shear rate from narrow slot approximation method (Aadnøy et al. 2009).

After calculating pressure loss gradient, total pressure loss is obtained, and it is presented in terms of equivalent circulating density by using Equation 11. Results of the sample scenarios are provided in Figure 19 and Figure 20.

$$ECD = \frac{\Delta P_f}{0.052*TVD} + MW \quad (11)$$

Based on the sample scenario results, it is observed that WBM#2 causes 17.5% additional ECD when compared with the steady state ECD, while this value is 3.1% for WBM#1 at 100 gpm. At 300 gpm, peak ECD almost doubles for WBM#1 (6.8%), meanwhile much larger pressure peak is observed for WBM#2 (42.4%).

Conclusions

Based on the experimental and theoretical works, observations and conclusions of this study can be summarized as:

- Both fluids used in this study show time-dependent and non-Newtonian fluid characteristics.
- SOT results indicate that both fluids form a gelled structure when they are not sheared.
- In reference to the shear stress peaks observed in SOTs, shear stress peak value increases with the increase in resting/waiting time.
- Both models converge to expected steady shear stress value when the fluid is sheared for a long period of time.
- OASTs show that both fluid represent viscoelastic behavior.
- The proposed models have a reasonable match with the experimental data for the early and peak times.
- As compared to the Viscoelastic model, Modified Leider & Bird model provides better match with the experimental data obtained by SOTs with respect to the post-peak stress behavior.
- In terms of model parameters, Modified Leider & Bird model requires less parameters to be obtained as compared to the Viscoelastic model. Moreover, one of the parameters of the former model is proposed to be gel strength data which could be collected with a field viscometer instead of using an advanced rheometer.
- Fluid displacement experiments show that the magnitude of pressure peaks increases with the increase in resting time as well as flow rate. WBM#2 (high yield fluid) causes higher pressure peaks when compared with WBM#1 (low yield fluid).
- Higher flow rate creates higher pressure peaks regardless of the fluid type with the same resting time.
- Like SOTs and gel strength data, fluid displacement tests show that the rate of structure development decreases by time. This can be seen in Figure 15 through Figure 18 constructed by highest pressure peak data obtained with flow loop experiments.
- The differences between measured values for different resting times are higher for WBM#2. This implies that WBM#2 has a higher rate of structure development.

Future Work

It is planned to run experiments with synthetic based fluids as well by implementing the same experimental procedures to be able to compare different type of fluid's behavior. Also, effect of shear rate on model parameters will be investigated. This is expected to provide a more comprehensive correlation which is a function of shear rate and resting time. Finally, the change in model parameters for aforementioned fluids will be evaluated.

Acknowledgments

This research was conducted at The University of Tulsa Drilling Research Projects (TUDRP). The investigator is sponsored by Turkish General Directorate of Mineral Research and Exploration (MTA).

Nomenclature

τ: *Shear stress, Pa*
τ_y *or* $\tau_{y(ss)}$*: Dynamic yield stress, Pa*
$\dot{\gamma}$: *Shear rate, 1/s*
t: Time, seconds
$\tau_y(t)$*: Time dependent yield stress, Pa*
τ_{gel}*: Static yield stress, Pa*
*K: Consistency index, Pa*s*^{m}
m: Flow behavior index
N: Generalized flow behavior index
G_0*: Shear modulus at zero shear, Pa*
G_1*: Shear modulus of a spring, Pa*
ECD: Equivalent circulating density, ppg
ΔP_f*: Annular frictional loss above the section of interest, psi*
TVD: True vertical depth, ft
MW: Mud weight, ppg
G_2*: Shear modulus of a Voigt material, Pa*
μ_1*: Viscosity of a Voigt material, Pa*s*
μ_2*: Viscosity of a dashpot, Pa*s*
τ_0*: Shear stress at zero time, Pa*
D_o*: Inner diameter of the wellbore, meter*
D_i*: Outer diameter of the drill string, meter*

References

1. Aadnøy, B. S., Cooper, I., Miska, S. Z., Mitchell, R. F., & Payne, M. L. 2009. Advanced Drilling and Well Technology. Society of Petroleum Engineers.
2. Altindal, M. C., Ozbayoglu, E., Miska, S., Yu, M., Takach, N., and May, R. 2017. "Impact of Viscoelastic Characteristics of Oil Based Muds/Synthetic Based Muds on Cuttings Settling Velocities." Proceedings of the ASME 2017 36th International Conference on Ocean, Offshore and Arctic Engineering. Volume 8: Polar and Arctic Sciences and Technology; Petroleum Technology. Trondheim, Norway. ASME. https://doi.org/10.1115/OMAE2017-62129.
3. Bekkour, K., Leyama, M., Benchabane, A., Scrivener, O. 2005. "Time-dependent rheological behavior of bentonite suspensions: An experimental study". Journal of Rheology 49, 1329.
4. Bjørkevoll, K. S., Rommetveit, R., Aas, B., Gjeraldstveit, H., Merlo, A. 2003. "Transient gel breaking model for critical wells applications with field data verification". Society of Petroleum Engineers. doi:10.2118/79843-MS.
5. Burgers, J.M. 1935. Mechanical Considerations, Model Systems, Phenomenological Theories, in Akademie van Wetenschappen, First Report on Viscosity and Plasticity, pp. 21–33.
6. Gandelman, R., Leal, R. A. F., Goncalves, J., Aragao, A. F. L., Lomba, R. F. T., & Martins, A. L. 2007. "Study on Gelation and Freezing Phenomena of Synthetic Drilling Fluids in Ultra Deep Water Environments." Society of Petroleum Engineers. doi:10.2118/105881-MS.
7. Leider, P. L., Bird, R. B. 1974. "Squeezing flow between parallel plates. I: Theoretical analysis," Ind. Eng. Chem. Fundam. 13, 336–341.
8. Maxey, J. 2007, "Thixotropy and Yield Stress Behavior in Drilling Fluids", AADE-07-NTCE-20 presented at the 2007 AADE National Technical Conference held in Houston, Texas, 10-12 April.
9. Mezger, T. G. 2011. The Rheology Handbook (3rd ed.). Hannover: Vincentz Network.
10. Steffe, J.F. 1996. "Rheological Methods in Food Process Engineering". Freeman Press, 2nd Edition, 294-348.
11. Steller, R. 2016. "Determination of the first normal stress difference from viscometric data for shear flows of polymer liquids". Rheol Acta 55:649–656. DOI 10.1007/s00397-016-0938-3.

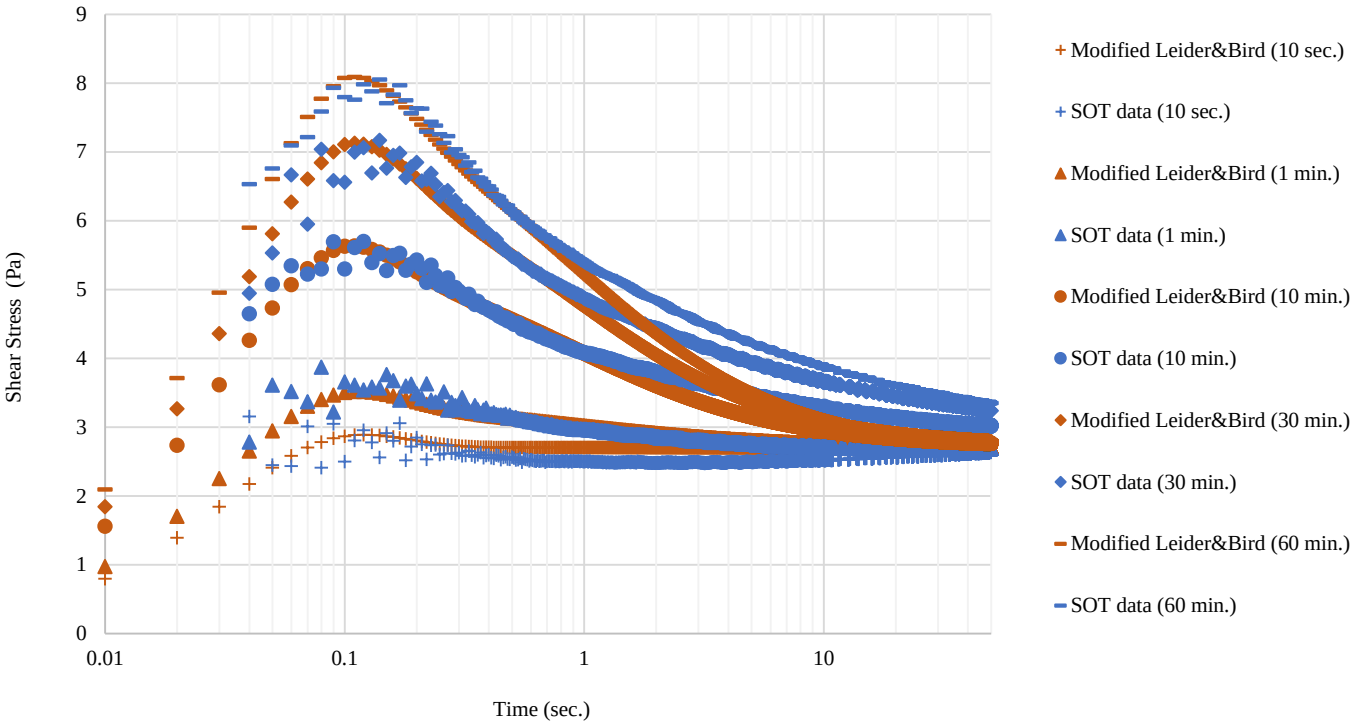

Figure 2 Modified Leider & Bird model and SOT data comparison at a shear rate of 10.22 s^{-1} with several resting times for WBM#1

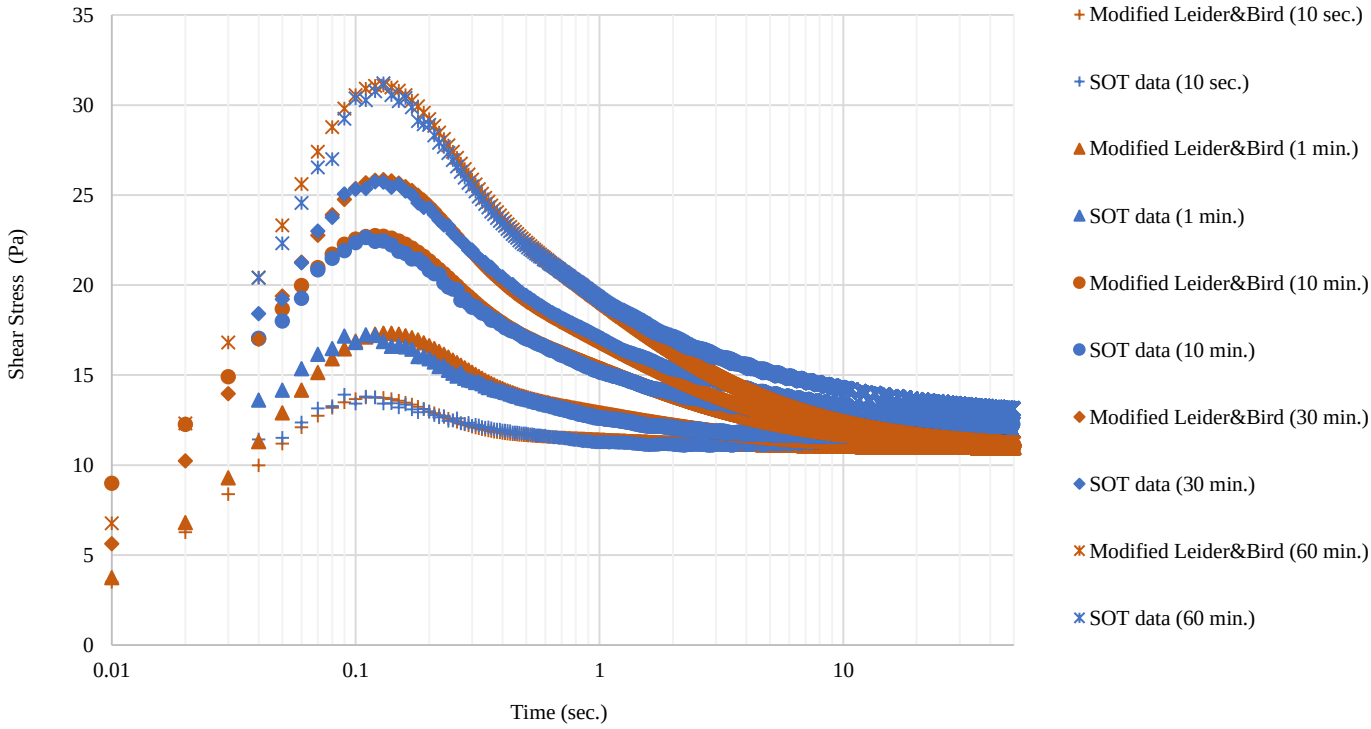

Figure 3 Modified Leider & Bird model and SOT data comparison at a shear rate of 10.22 s^{-1} with several resting times for WBM#2

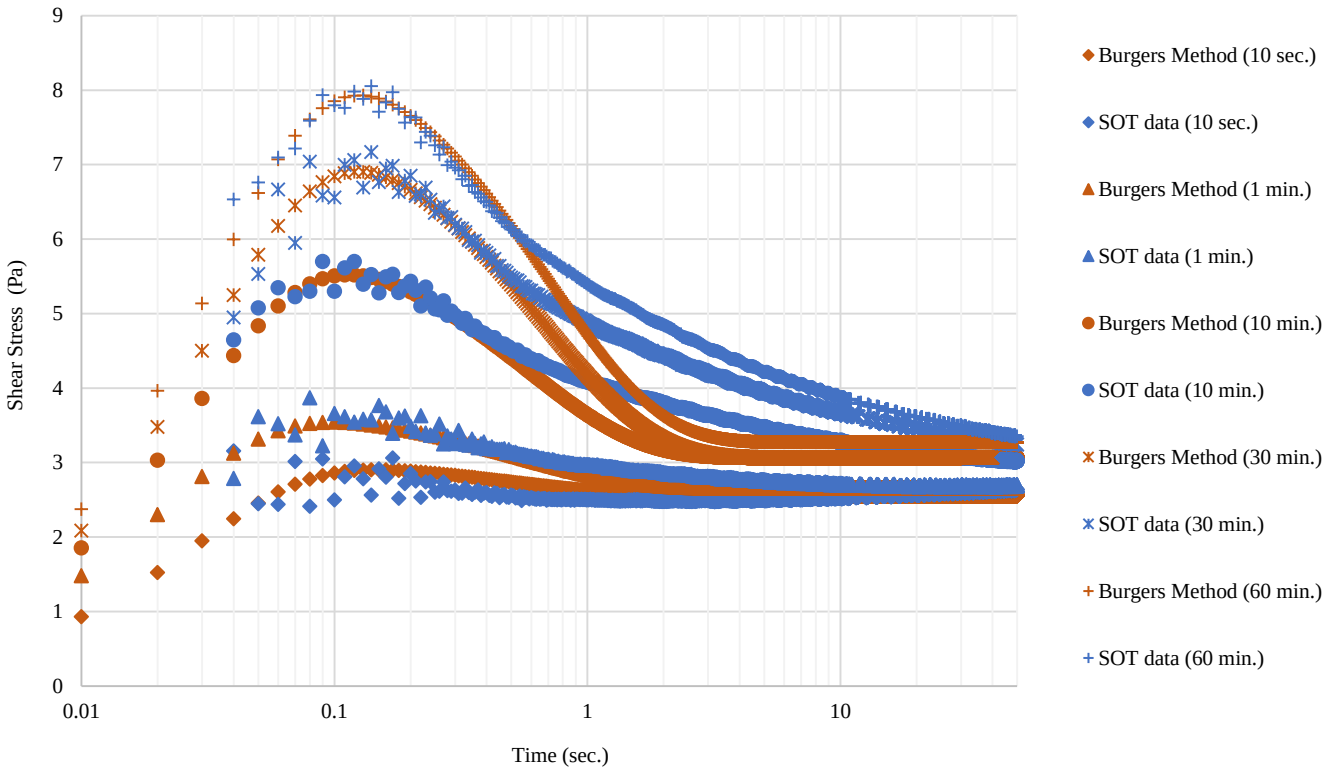

Figure 4 Burgers model and SOT data comparison at a shear rate of 10.22 s^{-1} with several resting times for WBM#1

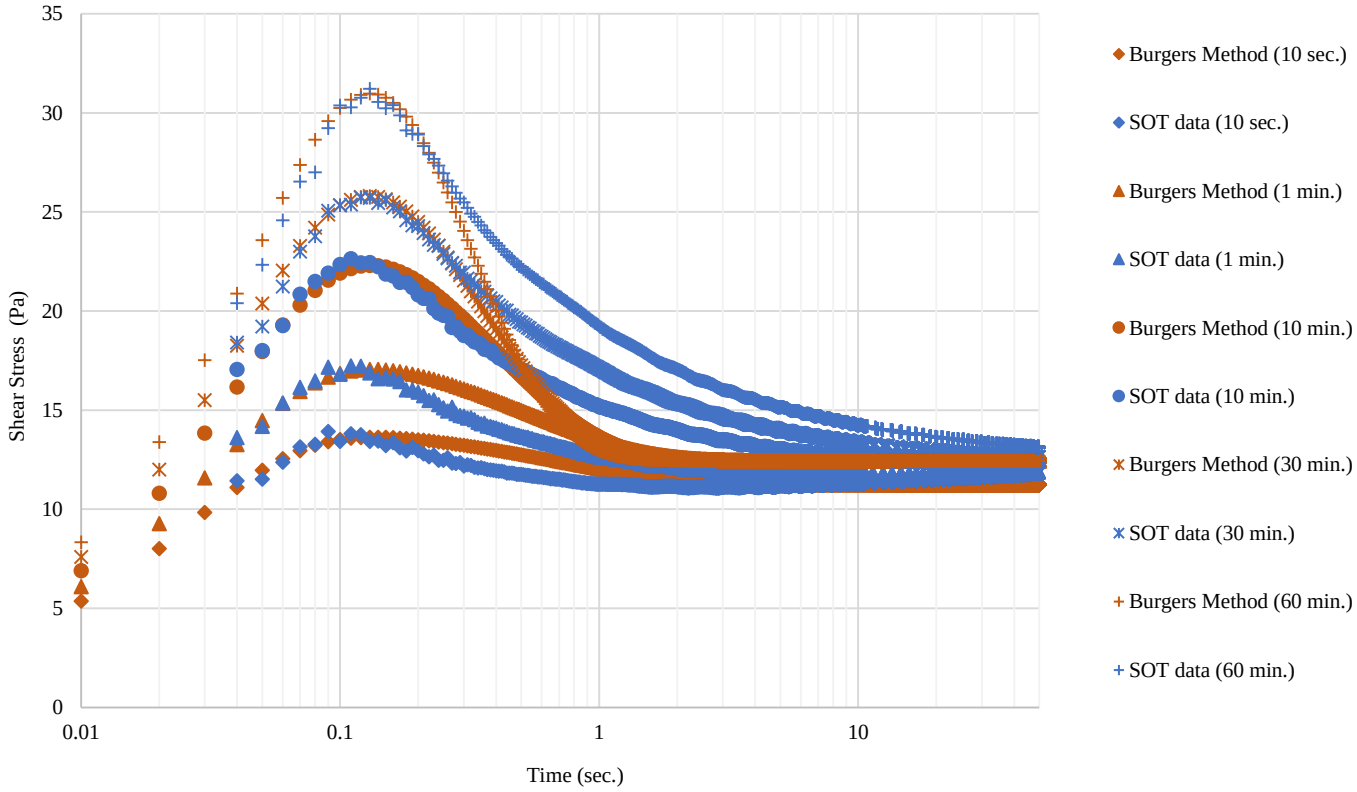

Figure 5 Burgers model and SOT data comparison at a shear rate of 10.22 s^{-1} with several resting times for WBM#2

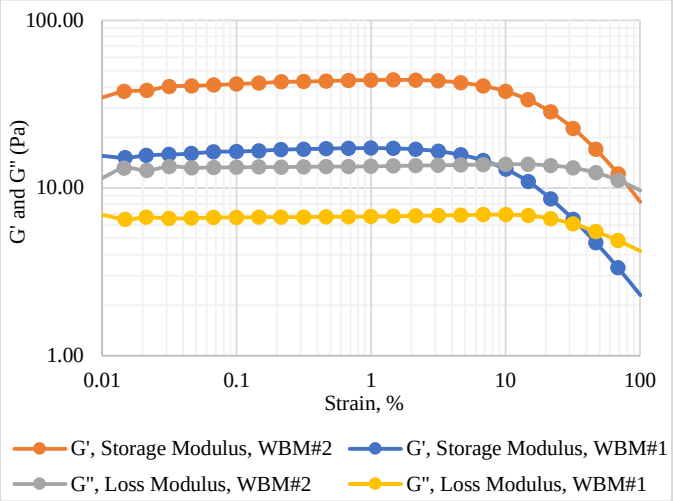

Figure 6 Oscillatory Amplitude Sweep Tests after steady state at 511 s^{-1} for WBM #1 and WBM #2 (w=10 s^{-1})

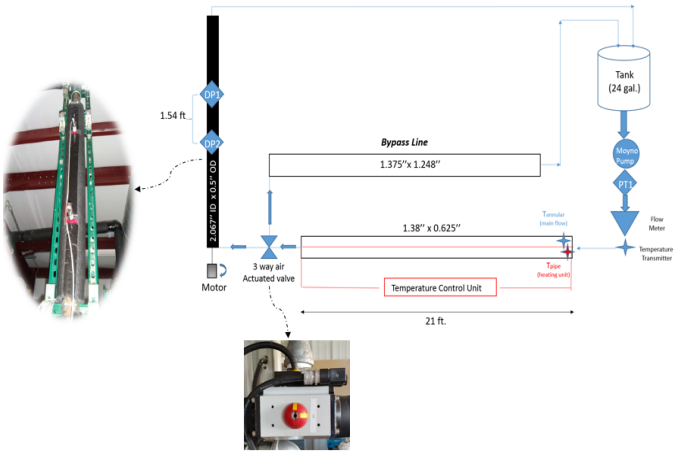

Figure 7 Simplified Schematic Diagram of TUDRP-DTF flow loop

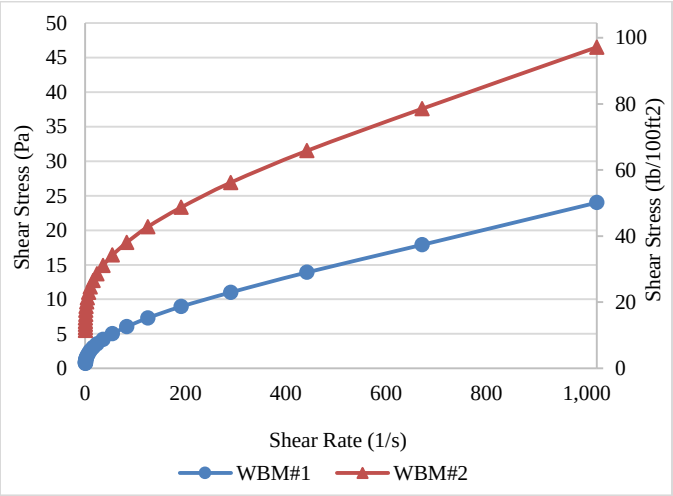

Figure 8 Comparison of flow curves of WBM #1 and WBM #2 fluids (Rheometer readings)

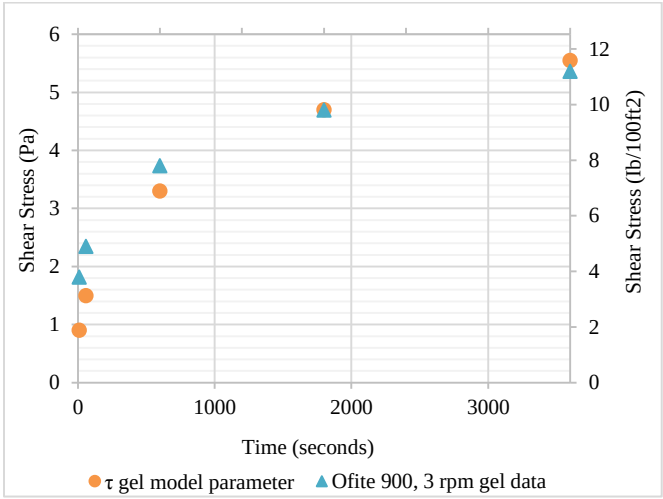

Figure 9 Comparison of viscometer 3 rpm gel strength and assumed static yield stress for different resting times, WBM#1

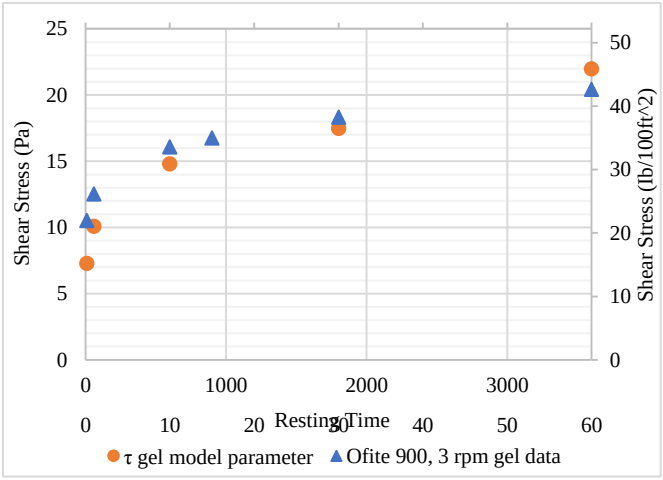

Figure 10 Comparison of viscometer 3 rpm gel strength and assumed static yield stress for different resting times, WBM#2

Table 4 Conventional viscometer readings for WBM#1 and WBM#2

Rotational speed (rpm)	Dial reading (lb/100 ft^2)	
	WBM#1	WBM#2
600	46	93.4
300	31.5	70.3
100	17.7	48
6	4.6	26
3	3.6	22.6
1	2.5	19.2

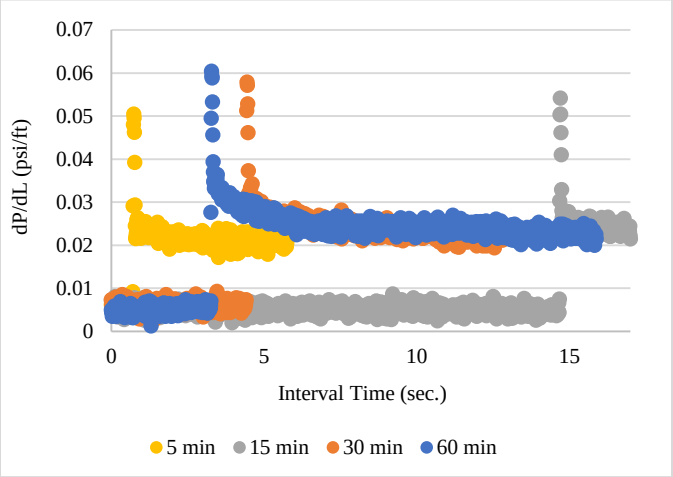

Figure 11 Transient pressure loss gradient for low yield fluid (WBM#1) at 5 gpm

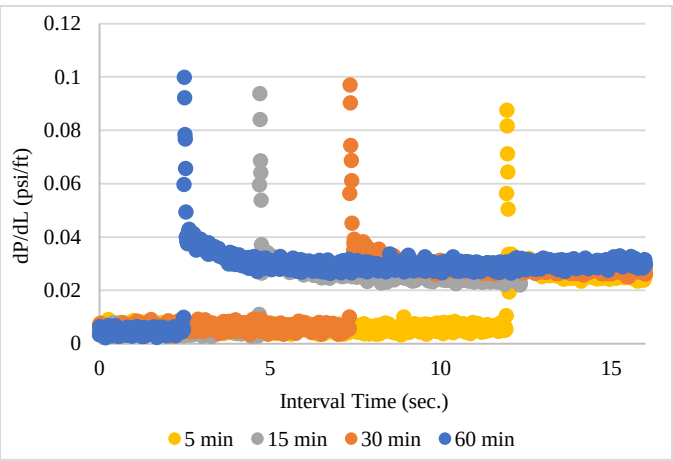

Figure 12 Transient pressure loss gradient for low yield fluid (WBM#1) at 10 gpm

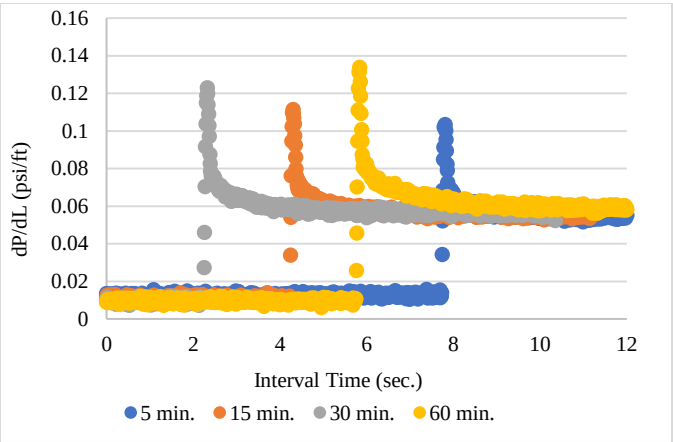

Figure 13 Transient pressure loss gradient for low yield fluid (WBM#2) at 5 gpm

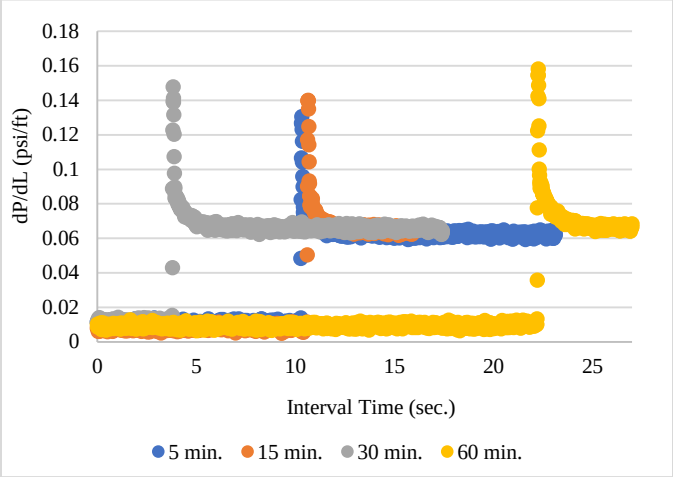

Figure 14 Transient pressure loss gradient for low yield fluid (WBM#2) at 10 gpm

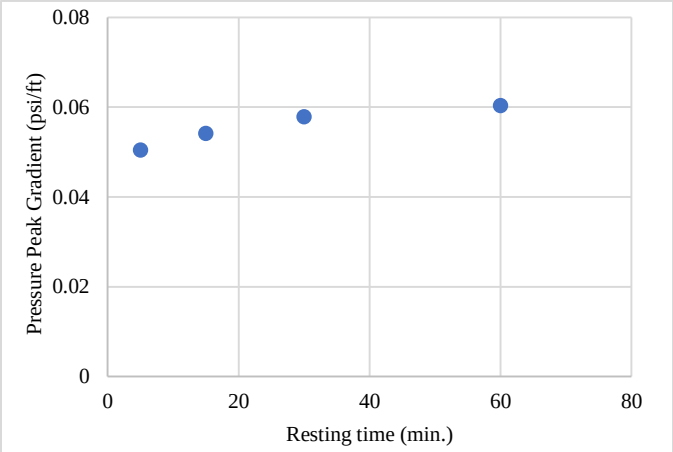

Figure 15 Measured pressure peak gradient with variety of resting times for WBM#1 at 5 gpm

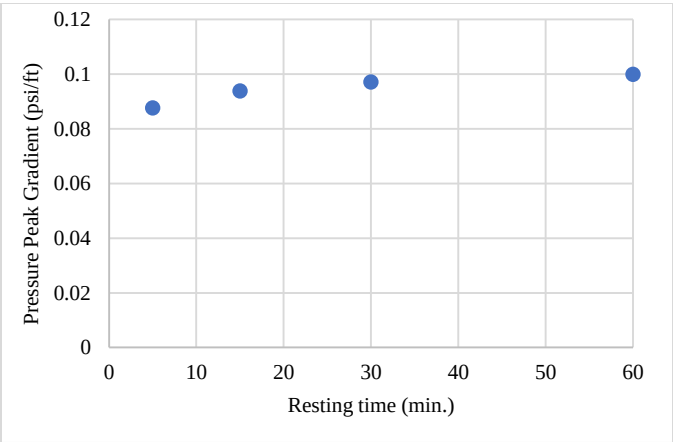

Figure 16 Measured pressure peak gradient with variety of resting times for WBM#1 at 10 gpm

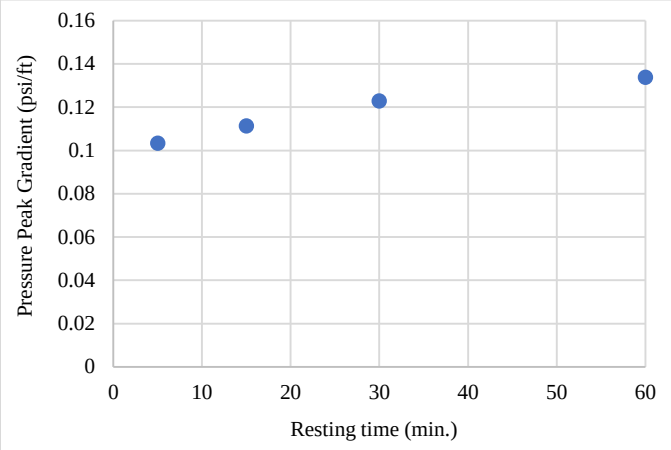

Figure 17 Measured pressure peak gradient with variety of resting times for WBM#2 at 5 gpm

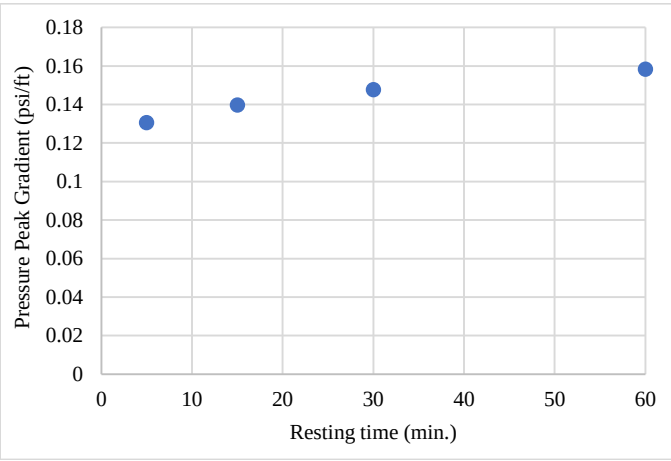

Figure 18 Measured pressure peak gradient with variety of resting times for WBM#2 at 10 gpm

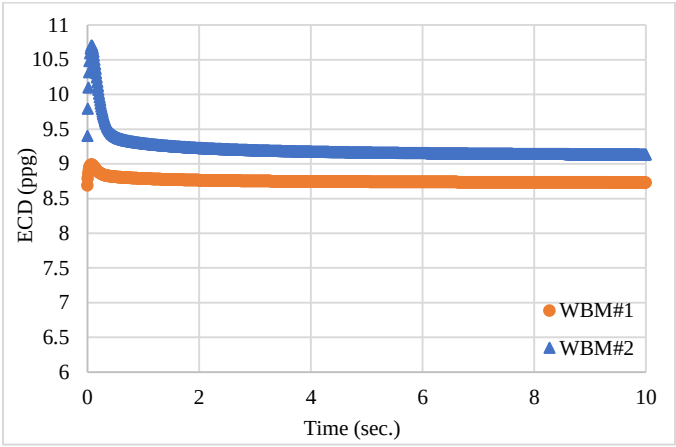

Figure 19 Sample scenario output with 100 gpm flow rate startup

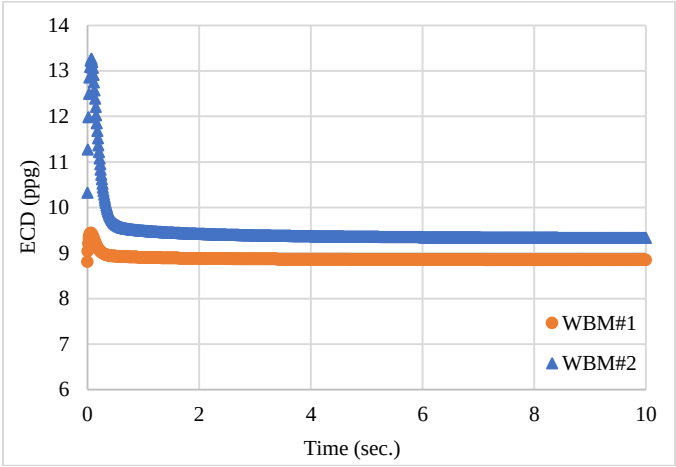

Figure 20 Sample scenario output with 300 gpm flow rate startup